

## ***Electronic Supplementary Information***

**Highly stable 3D porous HMOF with enhanced catalysis and fine color regulation by combination of d- and p-ions when compared with those of its monometallic MOFs**

Jiao Liu,<sup>a</sup> Ying Zhao,<sup>b</sup> Li-Long Dang,<sup>b</sup> Guoping Yang,<sup>\*a</sup> Lu-Fang Ma,<sup>\*ab</sup> Dong-Sheng Li<sup>c</sup> and Yaoyu Wang<sup>a</sup>

<sup>a</sup>*Key Laboratory of Synthetic and Natural Functional Molecule of the Ministry of Education, Shaanxi Key Laboratory of Physico-Inorganic Chemistry, College of Chemistry & Materials Science, Northwest University, Xi'an, 710127, Shaanxi, P. R. China.*

<sup>b</sup>*College of Chemistry and Chemical Engineering, Henan Key Laboratory of Function-Oriented Porous Materials, Luoyang Normal University, Luoyang 471934, P. R. China*

<sup>c</sup>*College of Materials and Chemical Engineering, Hubei Provincial Collaborative Innovation Center for New Energy Microgrid, Key Laboratory of Inorganic Nonmetallic Crystalline and Energy Conversion Materials, China Three Gorges University, Yichang 443002, P. R. China.*

E-mail: mazhuxp@126.com; ygp@nwu.edu.cn.

## Contents

Experimental section .....	1
The detail graphs of <b>1 - 3</b> .....	5
TGA of <b>1 - 3</b> .....	7
PXRD of <b>1 - 3</b> .....	8
IR of <b>1 - 3</b> .....	8
<sup>1</sup> H NMR spectrums .....	10
References .....	12

## Experimental Section

**Materials and Measurements.** In this study, all the materials were purchased for the experiments directly. The elemental analyses of C, H and N were tested with Perkin-Elmer 2400C elemental analyzer. Infrared spectra, powder X-ray diffraction data, thermogravimetric analyses and the solid state luminescent spectra were measured on Bruker EQUINOX-55 spectrophotometer in 4000–400 cm<sup>-1</sup> region, Bruker D8 ADVANCE X-ray powder diffractometer (Cu-K $\alpha$ , 1.5418 Å), NETZSCH STA 449C microanalyzer thermal analyzer and Hitachi F-4500 fluorescence spectrophotometer, respectively. <sup>1</sup>H NMR data were tested on a Bruker Ascend 400 (400 MHz) spectrometer.

**Crystal Structure Determination.** The single crystal X-ray diffraction were acquired on Bruker SMART APEX II CCD diffractometer with graphite monochromated Mo-K $\alpha$  radiation ( $\lambda = 0.71073$  Å) by using  $\phi/\omega$  scan technique. The diffraction data were corrected for Lorentz and polarization effects. The complexes were ensured by direct method and refined anisotropically on  $F^2$  by a full-matrix least-squares refinement with the *SHELXTL* program. The disordered molecules were processed by employing the SQUEEZE program of PLATON. The crystallographic, selected bond lengths and angles data of two complexes were listed in Table S2 and Table S3. CCDC: 1998756-1998758.

**Catalytic Experiment.** In the solvent-free environment, the epoxide substrates with different sizes of substituted groups were used as reactants to react with CO<sub>2</sub>, the activated **3** as catalyst and tetra-n-*tert*-butylammoniumbromide (TBAB) as co-catalyst. The catalytic reaction was carried out in a 5 mL Schlenk tube under stirring for 12 h (800 rpm). The formation of the desired carbonate was confirmed by <sup>1</sup>H NMR.

## Synthesis Experiment

**Synthesis of  $\{[Zn_{1.5}L(NMP)(H_2O)] \cdot H_2O\}_n$  (1).** Zn(NO<sub>3</sub>)<sub>2</sub>·H<sub>2</sub>O (0.1 mmol, 29.7 mg), H<sub>2</sub>L (0.05 mmol, 11.6 mg), H<sub>2</sub>O (5 mL) and NMP (3 mL) were mixed in 15 mL Teflon-lined stainless steel vessel, and then heated at 95 °C for 72 h. After that the vessel cooled to room temperature with a rate of 10 °C h<sup>-1</sup>, at last the colorless block crystals were obtained. Yield 92% (based on H<sub>2</sub>L). Elemental analysis of **1**, calculated (%): C, 36.20; H, 3.47; N, 15.07. Found: C, 36.11; H, 3.29; N, 15.31. FT-IR (KBr, cm<sup>-1</sup>, Figure S5): 3387 (m), 2885 (w), 1616 (s), 1573 (m), 1382 (m), 1427 (m), 1367 (m), 852 (w), 748 (m), 610 (w).

**Synthesis of  $[Pb_2L_2(H_2O)_2] \cdot H_2O\}_n$  (2).** Similar to the synthesis process of **1** expect that the metal were instead by Pb(NO<sub>3</sub>)<sub>2</sub>, the colorless needle-like crystals of **2** were acquired. Yield 93% (based on H<sub>2</sub>L). Elemental analysis of **2**, calculated (%): C, 23.66; H, 1.21; N, 12.26. Found: C, 23.41; H, 1.09; N, 12.79. FT-IR (Figure S5): 3430 (m), 2346 (m), 1676 (s), 1530 (s), 1410 (s), 1272 (s), 1246 (m), 1091(m), 816 (m), 756 (m), 559(w).

**Synthesis of  $\{[\text{PbZn}_{0.5}\text{L}(\text{H}_2\text{O})]\cdot0.5\text{NMP}\cdot\text{H}_2\text{O}\}_n$  (3).** Similar to the synthesis procedure of **1**, expect that add mixed metal ions of  $\text{Pb}(\text{NO}_3)_2$  (0.1 mmol, 33.1 mg) and  $\text{Zn}(\text{NO}_3)_2$  (0.05 mmol, 15.6 mg) to the Teflon-lined stainless steel vessel. The colorless crystals were obtained. Yield 84% (based on  $\text{H}_2\text{L}$ ). Elemental analysis of **3**, calculated (%): C, 22.10; H, 1.03. N, 11.45. Found: C, 22.02; H, 1.14. N, 10.20. FT-IR (Figure S5): 3415 (m), 1566 (s), 1515 (s), 1395 (s), 1265 (s), 1102 (m), 818 (s), 758 (m), 569 (m), 526 (w).

**Table S1.** Comparison of catalytic activities of HMOF **3** and the reported references.

Catalyst	T (°C)	P/MPa	t (h)	Yield (%)	Ref.
1 $\text{Zn}_4\text{Ln}_3\text{L}_4$	120	1.0	1	95	1
2 Ni-Co-MOF	80	1.2	8	96	2
3 VPI-100	90	1.0	6	96	3
4 COF-JLU7	40	0.8	48	92	4
5 HMOF <b>3</b>	25	0.1	12	98	<b>This work</b>

**Table S2.** Crystal Data and Structure Refinements of **1-3**.

Complex	<b>1</b>	<b>2</b>	<b>3</b>
Empirical formula	$\text{C}_{28}\text{H}_{32}\text{N}_{10}\text{O}_{14}\text{Zn}_3$	$\text{C}_{18}\text{H}_{11}\text{N}_8\text{O}_{10}\text{Pb}_2$	$\text{C}_9\text{H}_5\text{N}_4\text{O}_5\text{PbZn}_{0.5}$
Formula mass	928.74	913.73	489.04
Crystal system	Monoclinic	Triclinic	Monoclinic
Space group	P2(1)/n	P-1	C2/c
<i>a</i> [Å]	7.3787(9)	7.0192(10)	20.796(4)
<i>b</i> [Å]	15.3471(19)	12.1615(18)	22.171(4)
<i>c</i> [Å]	14.9299(18)	14.3322(19)	6.8392(12)
$\alpha$ [°]	90	66.712(4)	90
$\beta$ [°]	96.703(4)	85.198(4)	105.035(5)
$\gamma$ [°]	90	89.169(5)	90
<i>V</i> [Å <sup>3</sup> ]	1679.1(4)	1119.6(3)	3045.4(10)
Z	2	2	4
<i>D</i> <sub>calcd.</sub> [g·cm <sup>-3</sup> ]	1.837	2.710	2.133
$\mu$ [mm <sup>-1</sup> ]	2.212	15.094	11.868
<i>F</i> [000]	944	838	1792
$\theta$ [°]	2.654 - 25.000	2.825 - 25.421	2.737 - 24.997
Reflections collected	19977 / 2959	19780 / 4102	22431 / 2677
Goodness-of-fit on	1.038	1.047	1.086

Final [I>2σ(I)]	$R^{[a]}$ indices	$R_1 = 0.0233$	$R_1 = 0.0564$	$R_1 = 0.0566$
		$wR_2 = 0.0698$	$wR_2 = 0.1430$	$wR_2 = 0.1424$

<sup>a</sup>  $R_1 = \sum |F_o| - |F_c| / \sum |F_o|$ ,  $wR_2 = [\sum w(F_o^2 - F_c^2)^2 / \sum w(F_o^2)^2]^{1/2}$

**Table S3.** Selected bond distances (Å) and angles (°) of **1-3**.

Complex 1			
Zn(1)-O(1)	1.9599(16)	O(5)-Zn(1)-O(4)#2	93.65(7)
Zn(1)-O(5)	1.932(18)	O(1)-Zn(1)-O(5)	116.07(8)
Zn(1)-N(4)#1	1.9885(19)	O(1)-Zn(1)-O(4)#2	98.12(7)
Zn(1)-O(4)#2	1.9904(16)	O(5)-Zn(1)-N(4)#1	112.26(8)
Zn(2)-O(3)	2.0557(17)	O(3)-Zn(2)-O(3)#3	180.00(4)
Zn(2)-O(3)#3	2.0558(17)	O(3)#3-Zn(2)-O(6)#3	91.93(7)
Zn(2)-O(6)#3	2.1083(16)	O(3)#3-Zn(2)-O(6)#3	88.07(7)
Zn(2)-O(6)	2.1083(16)	O(3)-Zn(2)-O(6)	88.07(7)
Zn(2)-N(1)#3	2.131(2)	O(6)#3-Zn(2)-O(6)	180.00(9)
Zn(2)-N(1)	2.131(2)	O(3)-Zn(2)-N(1)#3	93.03(7)
O(4)-Zn(1)#4	1.9904(16)	O(3)#3-Zn(2)-N(1)#3	86.97(7)
N(4)-Zn(1)#5	1.9884(19)	O(6)#3-Zn(2)-N(1)#3	91.45(7)
N(1)#3-Zn(2)-N(1)	180.0	O(6)-Zn(2)-N(1)#3	88.55(7)
O(6)#3-Zn(2)-N(1)	88.55(7)	O(3)-Zn(2)-N(1)	86.97(7)
O(6)-Zn(2)-N(1)	91.45(7)	O(3)#3-Zn(2)-N(1)	93.03(7)
Complex 2			
Pb(2)-O(6)	2.554(11)	O(6)-Pb(2)-O(3)	65.4(3)
Pb(2)-O(3)	2.602(11)	O(6)-Pb(2)-O(4)#1	110.2(4)
Pb(2)-O(4)#1	2.564(11)	O(6)-Pb(2)-O(5)	50.2(3)
Pb(2)-O(5)	2.601(12)	O(6)-Pb(2)-N(3)#2	79.4(6)
Pb(2)-N(3)#2	2.72(3)	O(6)-Pb(2)-N(6)#3	67.7(3)
Pb(2)-N(6)#3	2.683(9)	O(3)-Pb(2)-N(3)#2	73.7(6)
Pb(1)-O(10)	2.640(10)	O(3)-Pb(2)-N(6)#3	70.2(3)
Pb(1)-O(6)	2.535(11)	O(4)#1-Pb(2)-O(3)	144.6(4)
Pb(1)-O(3)	2.493(10)	O(4)#1-Pb(2)-O(5)	71.7(4)
Pb(1)-N(7)#3	2.68(3)	O(4)#1-Pb(2)-N(3)#2	141.6(6)
O(4)-Pb(2)#4	2.564(11)	O(4)#1-Pb(2)-N(6)#3	75.8(3)

N(3)-Pb(2)#2	2.720(9)	O(5)-Pb(2)-O(3)	115.5(3)
N(6)-Pb(2)#3	2.683(9)	O(5)-Pb(2)-N(3)#2	90.1(6)
N(7)-Pb(1)#3	2.675(9)	O(5)-Pb(2)-N(6)#3	87.7(4)
O(6)-Pb(1)-N(7)#3	67.8(7)	N(6)#3-Pb(2)-N(3)#2	138.6(6)
O(3)-Pb(1)-O(10)	89.4(4)	O(10)-Pb(1)-N(7)#3	66.8(7)
O(3)-Pb(1)-O(6)	67.3(4)	O(6)-Pb(1)-O(10)	133.1(3)
O(3)-Pb(1)-N(7)#3	73.8(7)	Pb(1)-O(6)-Pb(2)	111.8(4)
Pb(1)-O(3)-Pb(2)	111.6(4)		

### Complex 3

Pb(1)-O(5)	2.438(11)	O(5)-Pb(1)-O(4)	78.0(3)
Pb(1)-O(4)	2.694(9)	O(5)-Pb(1)-O(2)#1	88.0(3)
Pb(1)-O(2)#1	2.478(10)	O(5)-Pb(1)-N(4)#2	77.8(3)
Pb(1)-N(4)#2	2.668(10)	O(5)-Pb(1)-O(3)#3	81.4(4)
Pb(1)-O(3)	2.602(10)	O(5)-Pb(1)-O(3)	79.5(4)
Pb(1)-O(3)#3	2.617(10)	O(2)#1-Pb(1)-O(4)	154.8(3)
Zn(1)-O(1)#4	1.931(9)	O(2)#1-Pb(1)-N(4)#2	82.9(3)
Zn(1)-O(1)#5	1.931(9)	O(2)#1-Pb(1)-O(3)#3	80.1(3)
Zn(1)-N(1)	1.984(10)	O(2)#1-Pb(1)-O(3)	148.6(3)
Zn(1)-N(1)#6	1.984(10)	N(4)#2-Pb(1)-O(4)	73.9(3)
O(2)-Pb(1)#7	2.478(10)	O(3)-Pb(1)-O(4)	49.0(3)
N(4)-Pb(1)#2	2.668(10)	O(3)#3-Pb(1)-O(4)	117.6(3)
O(1)-Zn(1)#5	1.931(9)	O(3)#3-Pb(1)-N(4)#2	153.4(4)
O(3)-Pb(1)#3	2.617(9)	O(3)-Pb(1)-N(4)#2	121.6(3)
O(1)#4-Zn(1)-N(1)	116.5(4)	O(3)-Pb(1)-O(3)#3	69.6(3)
O(1)#5-Zn(1)-N(1)#6	116.5(4)	O(1)#4-Zn(1)-O(1)#5	95.1(5)
O(1)#4-Zn(1)-N(1)#6	109.0(4)	O(1)#5-Zn(1)-N(1)	109.0(4)
Pb(1)-O(3)-Pb(1)#3	110.4(3)	N(1)-Zn(1)-N(1)#6	110.1(6)

Symmetry codes in **1**: #1: -x+1/2, y+1/2, -z+1/2; #2: -x+3/2, y+1/2, -z+1/2; #3: -x+2, -y+1, -z+1; #4: -x+3/2, y-1/2, -z+1/2; #5: -x+1/2, y-1/2, -z+1/2. Symmetry codes in **2**: #1: x-1, y, z; #2: -x+1, -y+1, -z+1; #3: -x, -y, -z+2; #4: x+1, y, z. Symmetry codes in **3**: #1: -x+1/2, y+1/2, -z+1/2; #2: -x+1/2, -y+3/2, -z+1; #3: -x+1/2, -y+3/2, -z; #4: x, -y+1, z-1/2; #5: -x+1, -y+1, -z+1; #6: -x+1, y, -z+1/2; #7: -x+1/2, y-1/2, -z+1/2.

The detail graphs of 1 - 3

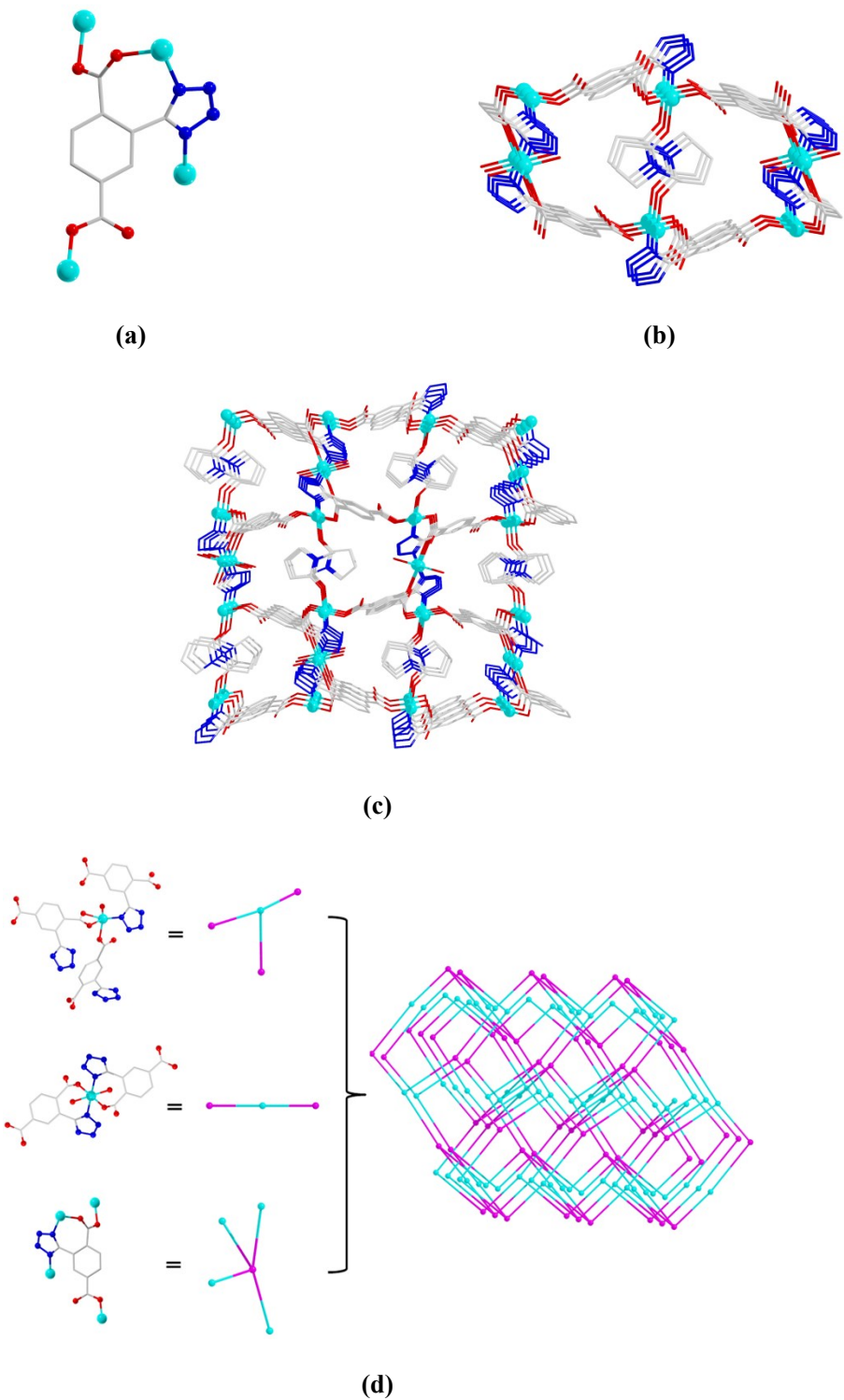


**Figure S1** (a) The coordination mode of  $L^{2-}$  ligands in **1**; (b) 1D pore structure; (c) 3D dense framework of **1**; (d) Schematic representation of a binodal (2,3,4)-connected *ins* net of **1**.

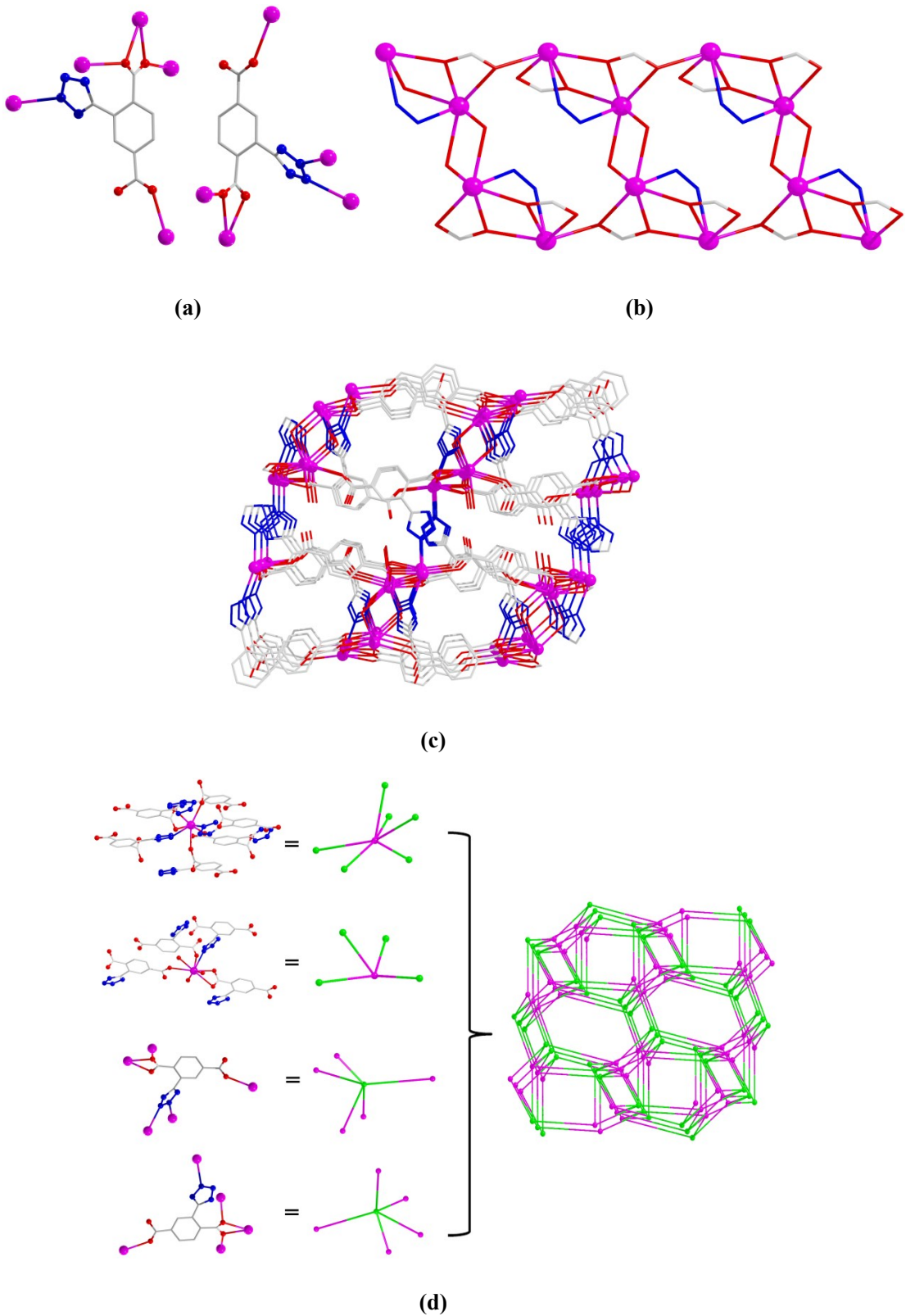


**Figure S2** (a) The coordination modes of  $\text{L}^{2-}$  ligands in **2**; (b) 1D chain; (c) 3D dense framework of **2**; (d) Schematic representation of a tetra-nodal (4,5,5,6)-connected topology net of **2**.

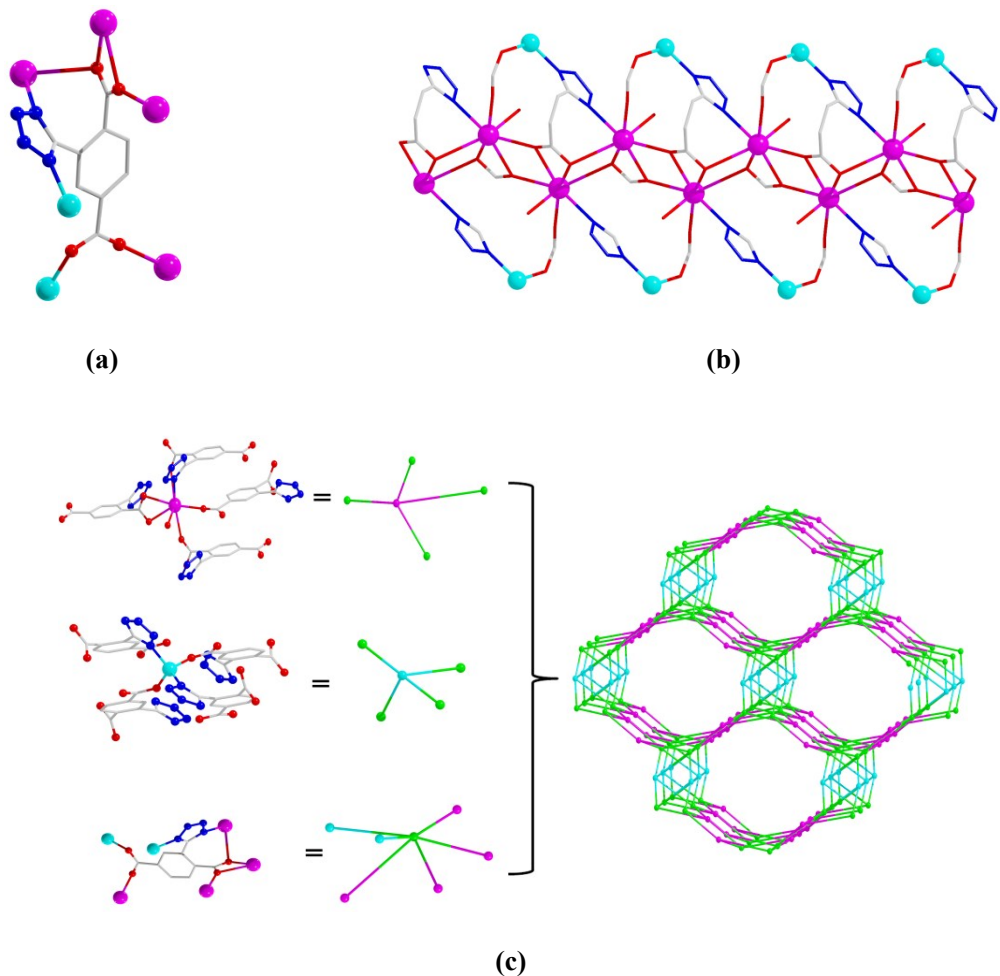


**Figure S3** (a) The coordination mode of  $L^{2-}$  ligands in **3**; (b) 1D bimetallic chain in **3**; (c) Schematic representation of a trinodal (4,4,6)-connected topology net of **3**.

#### TGA of **1 - 3**

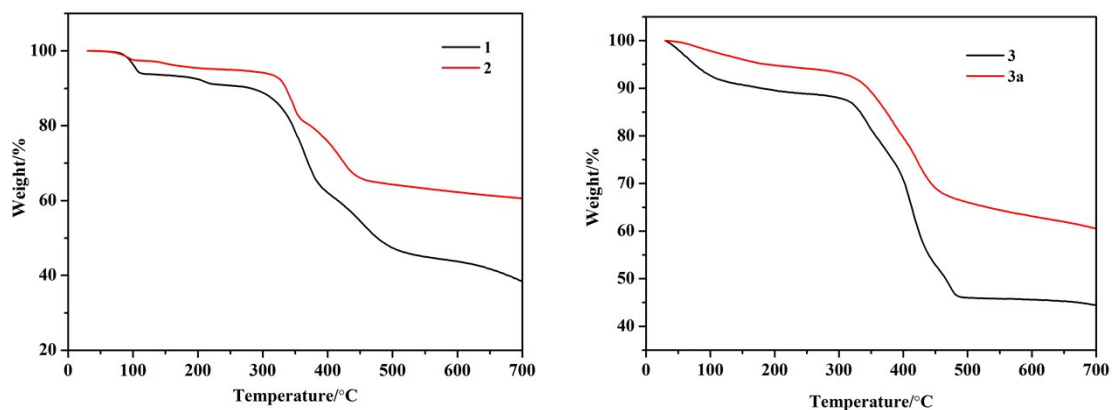


**Figure S4** TGA curves of **1 - 3**

### PXRD of 1 - 3

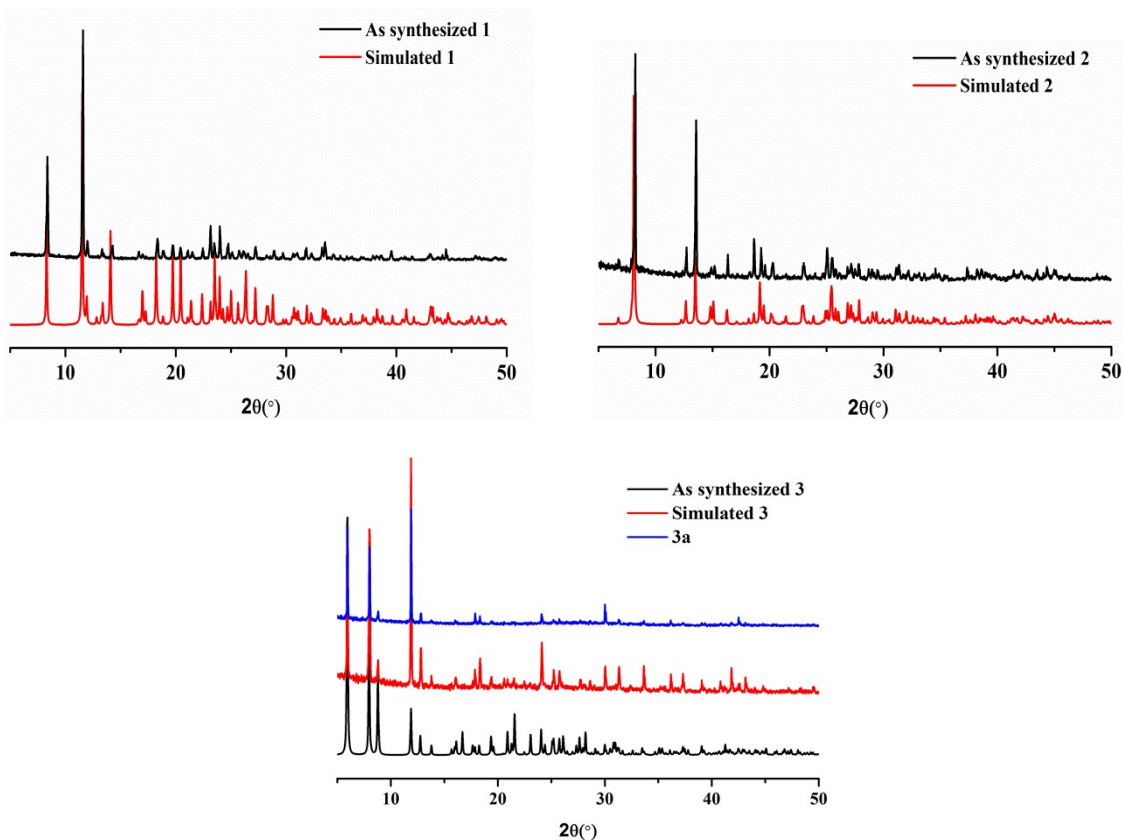


**Figure S5** PXRD patterns of the as-synthesized 1 - 3.

### IR of 1 - 3

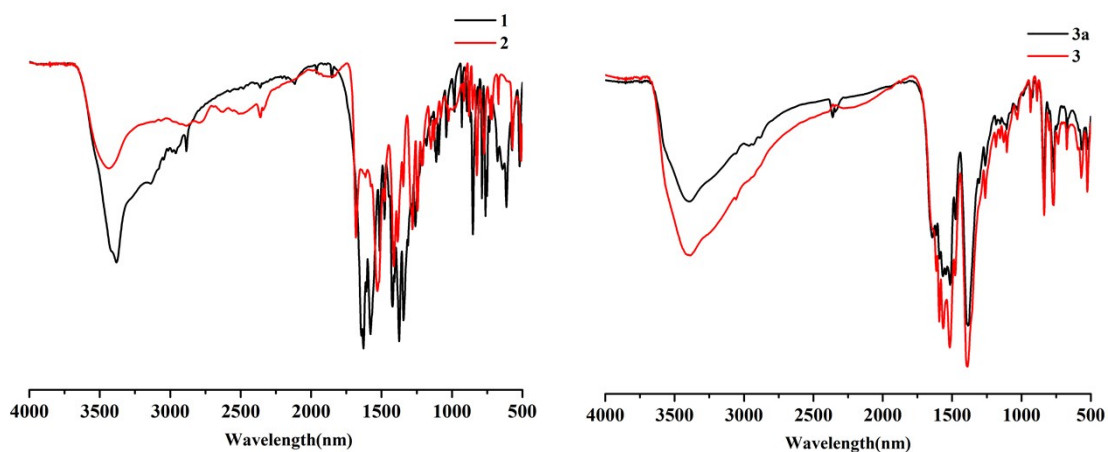
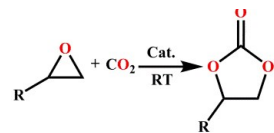
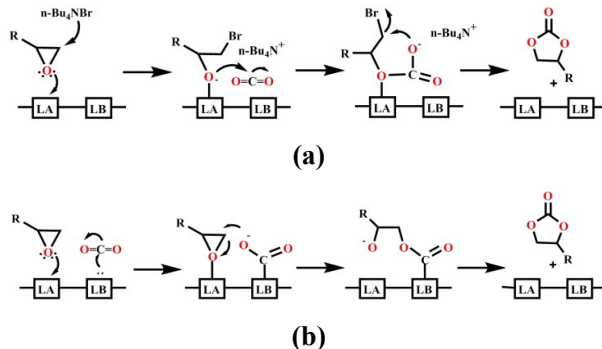


**Figure S6** The FT-IR spectra of the as synthesized 1 - 3 and desolvated 3 (3a).



**Scheme S1** Reaction scheme of the cycloaddition of  $\text{CO}_2$  to epoxides catalyzed by **3a**.



**Scheme S2** The proposed mechanism of the HMOF **3**-catalyzed  $\text{CO}_2$  cycloaddition reaction.

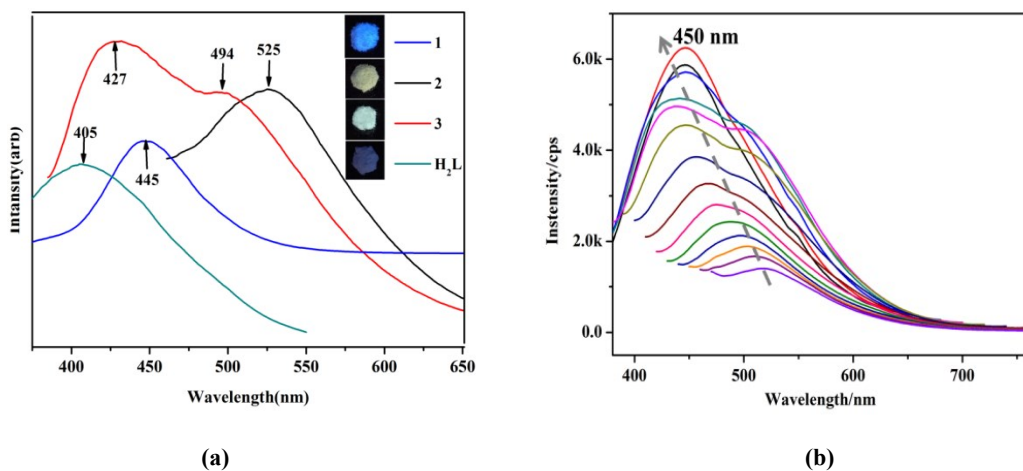


**Figure S7** (a) Photograph the solid-state emission spectra of **1** - **3** and free  $\text{H}_2\text{L}$  at room temperature. (b) The solid state emission spectra of **3** under different excitation ranges from 320 to 450 nm with an interval of 10 nm.

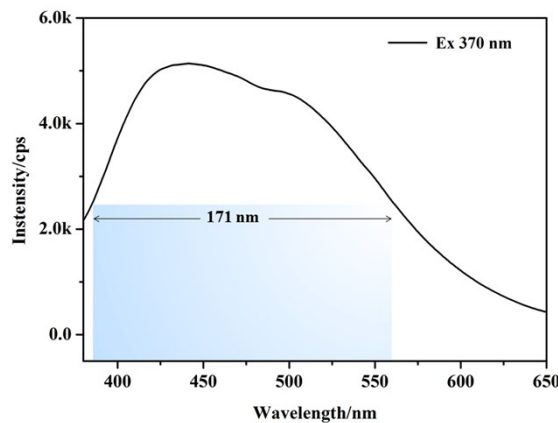
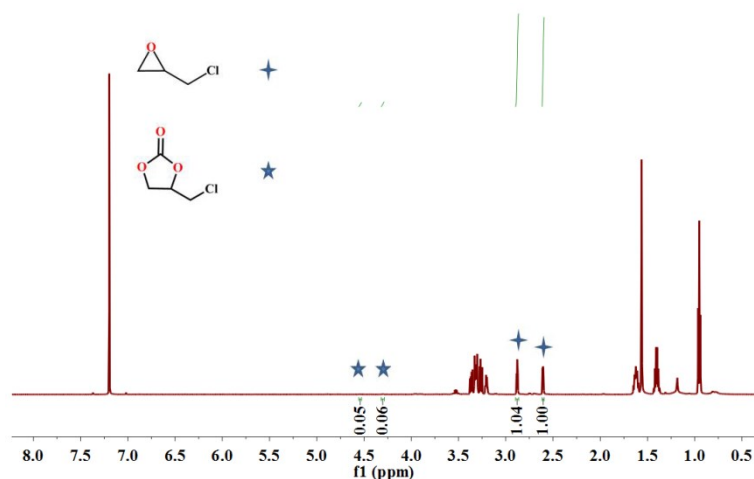
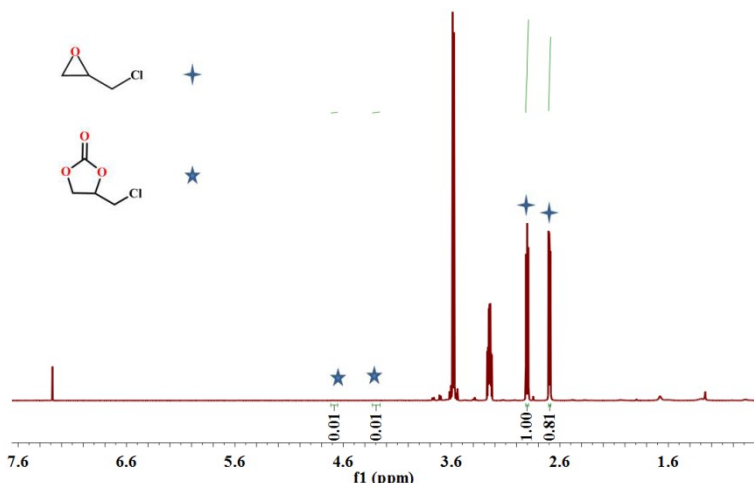


**Figure S8** The full width at half maximum (FWHM) of **3**.

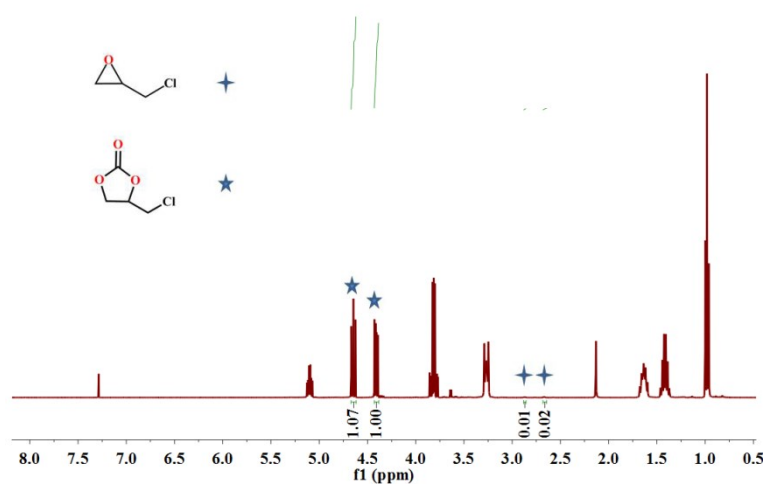
## **<sup>1</sup>H NMR spectra**



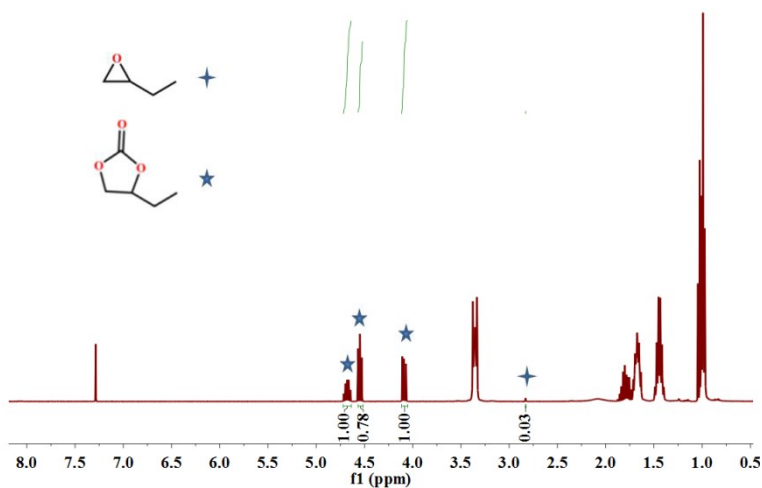
<sup>1</sup>H NMR spectrum of cyclic carbonate with **3a** (Table 1, entry 1).



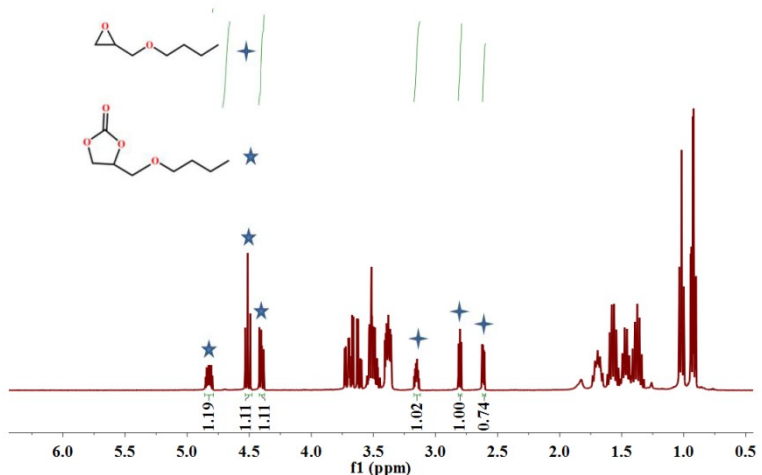
<sup>1</sup>H NMR spectrum of cyclic carbonate with **3a** (Table 1, entry 2).



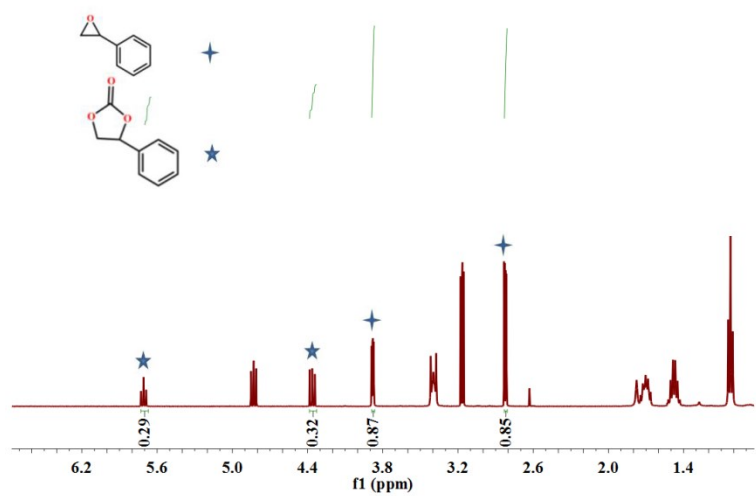
<sup>1</sup>H NMR spectrum of cyclic carbonate with **3a** (Table 1, entry 3).



<sup>1</sup>H NMR spectrum of cyclic carbonate with **3a** (Table 1, entry 4).



<sup>1</sup>H NMR spectrum of cyclic carbonate with **3a** (Table 1, entry 5).



<sup>1</sup>H NMR spectrum of cyclic carbonate with **3a** (Table 1, entry 5).

### References

1. L. Wang, C. Xu, Q. Han, X. Tang, P. Zhou, R. Zhang, G. Gao, B. Xu, W. Qin and W. Liu, *Chem Commun.*, 2018, **54**, 2212-2215.
2. J. F. Kurisingal, R. Babu, S.-H. Kim, Y. X. Li, J.-S. Chang, S. J. Cho and D.-W. Park, *Cata. Sci. Tech.*, 2018, **8**, 591-600.
3. J. Zhu, P. M. Usov, W. Xu, P. J. Celis-Salazar, S. Lin, M. C. Kessinger, C. Landaverde-Alvarado, M. Cai, A. M. May, C. Slebodnick, D. Zhu, S. D. Senanayake and A. J. Morris, *J. Am. Chem. Soc.*, 2018, **140**, 993-1003.
4. Y. Zhi, P. Shao, X. Feng, H. Xia, Y. Zhang, Z. Shi, Y. Mu and X. Liu, *J. Mater. Chem. A*, 2018, **6**, 374-382.